Nuclear Physics B (Proc. Suppl.) 12 (1990) 201–218
North-Holland

THE SMALL-X LIMIT AND THE POMERON IN QCD

Jochen BARTELS

II. Institut für Theoretische Physik, Universität Hamburg

A theoretical overview is given of our present understanding of the small-x limit in deep-inelastic ep-scattering and its connection with the Pomeron in QCD. I also discuss a few phenomenological questions which will be relevant for HERA physics.

1. INTRODUCTION

Interest in the small-x region of structure function comes from both the experimental and theoretical sides. HERA will be the first machine which can measure the proton structure function in x down to 10^{-4}. Since existing data have not gone further than 10^{-2}, this opens a new and so far unexplored kinematic range for testing QCD. In purely hadronic reactions, perturbative QCD calculations of inclusive jet-cross sections (e.g. minijets) are becoming increasingly sensitive to the behavior of structure functions at very low x-values. From the theoretical point of view, the region of very small x-values boarders the Regge-limit which is still waiting for a satisfactory QCD-based high-energy theory. Whereas there is little doubt that the main features of hadron-hadron scattering in the Regge limit are due to nonperturbative aspects of QCD, deep inelastic scattering at moderately low x-values is well-described by perturbative QCD. The limit $x \to 0$ therefore takes us from perturbative QCD into nonperturbative dynamics, and any improvement in our understanding of the small-x region will be of help for advancing in the Regge limit.

This talk is mainly a review and tries to cover both the main theoretical aspects and the present phenomenological situation. Since quite a few features of the small-x physics have been discussed and summarized[1-3] in the two Snowmass meetings and the Madison conference[4], I will try to concentrate on those aspects which either have not yet been emphasized so much or where some new work has

0920-5632/90/$03.50

been done since. In the first (theoretical) part I will mainly explain that our present understanding of the Regge-limit in QCD is fully consistent with the ideas of Gribov, Levin, and Ryskin[5] on improving the standard QCD description in the small-x region: the fan-diagrams, which these authors propose as an improvement of the standard QCD-ladders, smoothly transform into the Reggeon field theory which describes the Regge-limit. In the second part I discuss a few phenomenological questions: (i) how small has x to be in order to "feel" the presence of these fan-diagrams[2]. As I will explain, there is evidence that $x = 10^{-3} \ldots 10^{-4}$ may very well see these effects, but serious theoretical efforts are needed for performing numerical calculations (this conclusion may be somewhat different from those drawn at the Snowmass meetings). (ii) How well is the $1/\sqrt{x}$ behavior of $x\,G(x,Q^2)$ (gluon structure function) theoretically established? (iii) How much does perturbative QCD tell us about the Pomeron structure function of Ingelman and Schlein? I will argue that this structure function is closely related to other, already known structure functions and, in certain kinematic regions, even computable in perturbative QCD.

2. THEORETICAL BACKGROUND

The particular interest in the small-x region is due to the fact that the standard QCD evolution picture[6] of the structure function breaks down when x becomes too small. The momentum-weighted gluon structure function (as given by the QCD ladder diagrams (Fig. 1) or, equivalently, by the Lipatov-Altarelli-Parisi equations) has the small-x behavior:

$$x\,G(x,\xi) \sim \exp\sqrt{16N\xi \ell n\frac{1}{x}} \qquad (1.1)$$

with $\xi = \ell n\left[(\ell n\, Q^2/\Lambda^2)/(\ell n\, Q_0^2/\Lambda^2)\right]$, $x = Q^2/2pq$. It grows faster than any power of $\ln(1/x) \sim \ln(s/Q^2)$ and thus violates the Froissart bound. Phrased in a more intuitive language, the small-x problem arises because the density of slow gluons grows too strongly. In the standard QCD description (single ladder approximation, Fig. 1) the whole cascade of parton decays starts from only one of the constituents at low momentum scale, and the interaction with one of the other virtual clouds of partons is unimportant as long as x is not too small. It is only when, in deep inelastic scattering, the photon tries to find a quark with very small x that the single-ladder approximation (1.1) needs modifications: interactions of different chains of parton decays (ladders) lead to a slower increase of the gluon structure function in $1/x$ than given by (1.1). When $1/x$ goes to infinity (at fixed Q^2) we must, of course, enter the Regge-limit of QCD, the (nonperturbative) Pomeron. The small-x limit, therefore, provides a continuous entrance into the Regge-limit, starting from a perturbative beginning and ending at a nonperturba-

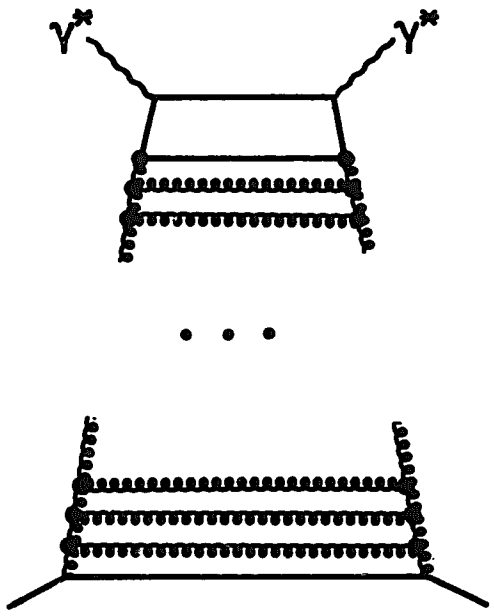

Fig. 1: QCD "standard" ladder diagrams for the structure function in deep-inelastic scattering. For small x only gluons are important.

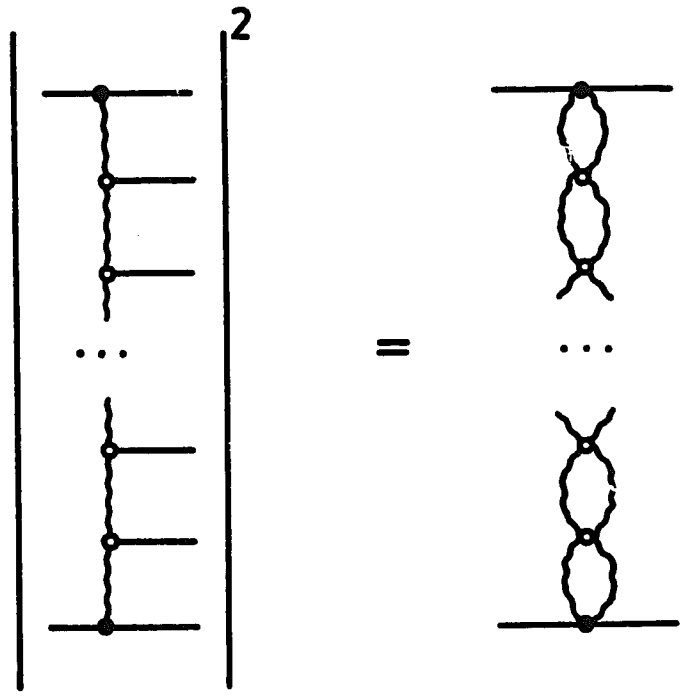

Fig. 2: QCD diagrams for the leading-lns Pomeron. The wavy lines denote reggeized gluons, the open circles stand for momentum dependent reggeon interaction vertices.

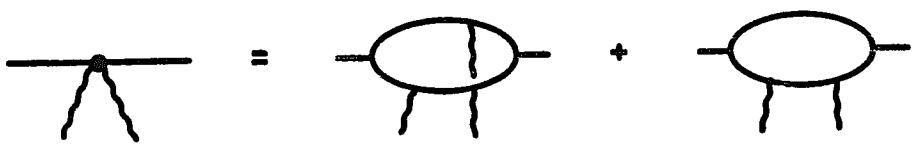

Fig. 3: Scattering of heavy-flavor mesons: coupling of the leading-lns Pomeron to the $q\bar{q}$-system.

tive end, and $^1/x$ acts as a control parameter. The perturbative QCD analysis of the small-x region of deep inelastic scattering has been thoroughly examined by Gribov, Levin and Ryskin[5]. Rather than repeating their results I will try to outline how our present (incomplete) understanding of the Regge-limit of QCD supports and perfectly matches with their improvement ideas. For this I have to review briefly a few results of the Regge-limit (although many of these facts have already been mentioned in Alan White's talk), and I will then return to a comparison with the small-x physics.

Although most of us are fully convinced that the Regge-limit of QCD (i.e. the structure of the Pomeron) is governed by nonperturbative confinement dynamics, there seems to be no better method for analyzing the Pomeron than by starting from its perturbative content and then extending into the region of small intrinsic transverse momenta where perturbation theory becomes unreliable. In this process of continuation formal aspects of unitarity in both the direct and the cross channel are of central importance. Logically, our present status of understanding can be summarized in three parts: (i) the leading-lns Pomeron (often referred to as "Lipatov ladders"), and its defects; (ii) unitarization or, equivalently, the derivation of a complete reggeon field theory; (iii) attempts to study the spectrum and the phase structure of this field theory.

Let me start with a brief review of the leading-lns Pomeron. Its origin are many-gluon production amplitudes in the multiregge-limit[7-13] (Fig. 2). In order to justify the use of perturbation theory in α_s one needs a large momentum scale. As an example, one might consider the scattering of two heavy-flavour mesons[10], where the coupling of the two (reggeized) gluons in the t-channel to the meson has to be gauge invariant (Fig. 3). The scale for momenta is then set by the mass of the heavy quark, m_q. For this process, the diagrams of Fig. 2 then represent those terms of the perturbation expansion which, for each power of $\alpha_s(m_q^2)$, provide the maximal power of $\ell n\ s$. The expansion parameter in the sum of all diagrams of Fig. 2 is $\alpha_s(m_q^2) \cdot \ell n(s/m_q)$ which has to be less than 1. As it is well-known, the leading high-energy behavior of these diagrams is described by a fixed-cut singularity in the angular momentum plane to the right of $j = 1$ (for SU(N) the location is $j = 1 + \alpha_s \frac{4N\ln 2}{\pi}$). Both the nature of this singularity (a fixed cut instead of a moving pole in the angular momentum plane) and its location (which leads to a violation of the Froissart bound by a power of s) are unacceptable. A closer look at the dynamical origin of this singularity shows, from the theoretical point of view, what goes wrong in this approximation. The diagrams of Fig. 2, to any finite order in α_s, are perfectly finite in both the ultraviolet and the infrared region, but when more and more iterations of them in the t-channel are taken into account, that part of the internal

phase space which is responsible for the leading j-plane singularity extends more and more into the ultraviolet and infrared region. In the leading-lns approximation, however, neither of them is treated quite correctly: in the UV-region, this approximation does not generate a momentum dependent coupling constand $\alpha_s(k^2)$, but keeps $\alpha_s(m_q^2)$ fixed. In the IR-region, $\alpha_s(k^2)$ grows and perturbation theory is unreliable. The first deficiency can be cured rather easily by introducing by hand the running coupling constant, whereas the latter is more serious, due to our lack of understanding the dynamics of confinement. Lipatov[11] has given an argument that, by taking into account asymptotic freedom in the UV-region and by modifying the IR-behavior of the Feynman amplitudes to account for nonperturbative effects, the previous fixed-cut resolves into a string of poles. Very unfortunately, however, the rightmost one of them still sits to the right of $j = 1$. It is thus clear that this leading-lns Pomeron - even with such corrections - is an unacceptable approximation. The fixed-cut singularity at $j > 1$ (or the string of poles, in the modified version) is an artifact of this approximation and will not be present in the final theory. What is still missing is s-channel unitarity.

When trying to restore s-channel unitarity it is crucial to consider not only $2 \to 2$ scattering amplitudes but also inelastic amplitudes. Unitarity must be satisfied in all subenergies. As to a practical procedure[14], one wants to construct a scattering matrix T whose elements are the $T_{n\to m}$ in multiregge limits. In order to fulfill the unitarity equation $T - T^+ = iTT^+$ one starts with the $T_{n\to m}$ in the leading-lns approximation and then solves the nonlinear unitarity matrix equation in an iterative way. The leading-lns Pomeron was just a first example of this procedure, other examples are shown in Figs. 4 and 5. The result of this scheme is a complete reggeon field theory with general $n\to m$ reggeon vertices (obeying signature conservation rules). The reggeized gluon plays the rôle of the elementary field, and the Pomeron is the leading bound state of 2, 4, 6, ... reggeons. This is not the place to go into further details, but a few remarks should be made. (i) The unitarization procedure makes heavy use of S-matrix and Regge-theory. In order to avoid problems that are associated with the presence of massless particles one conveniently uses the Higg's mechanism to give the gluons a mass. At the end of all calculations this IR-cutoff has to be removed: there is evidence (although not a strict proof) that this regularization scheme is correct, even beyond perturbation theory. (ii) By construction, this reggeon field theory satisfies asymptotic s-channel unitarity and partial-wave t-channel unitarity. While the gluon mass is still nonzero, this set of $n\to m$ scattering amplitudes is the first complete and self consistent realization of S-matrix postulates and

Regge-theory. An important ingredient are "bootstrap equations", the simplest example of which has been found by Lipatov et al. (iii) For any attempt to study the dynamics of this reggeon field theory it seems indispensable to know the detailed form of the general n→m reggeon vertex: this has not yet been worked out. (iv) The examples of Figs. 4 and 5 and our emphasis on unitarity in subenergies of inelastic amplitudes show that there is no evidence for any simple eikonal picture.

After the removal of the gluon mass this reggeon field theory (i.e. the sum of all diagrams which define reggeons and their interaction vertices) represents the minimal set of terms which are required by unitarity. To find out what its high energy behavior is (e.g. the leading singularity in the j-plane) remains as the third and final step. There are a few features which make a study of this field theory rather difficult: it has infinitely may interaction vertices, and a priori there is little justification that some of them might be less important than others. The vertices are momentum-dependent functions (i.e. nonlocal operators), and this momentum dependence is essential for internal consistency (e.g. reggeization of the gluons). Moreover we are not interested in some finite renormalization of the reggeon (gluon) fields but in the bound state spectrum in the even-signature, color zero t-channel. The hardest part of the problem, however, lies in the infrared region of the internal momentum integrals. Since the effective coupling constant is large, it seems likely that the expressions obtained from perturbation theory (although it may turn out they are infrared finite) have to be modified by nonperturbative effects (cf. the discussion of the leading-lns Pomeron). For this we clearly need to improve our understanding of confinement dynamics, and it may turn out that the Pomeron problem can be settled only after we have solved the confinement problem (see, however, another point of view presented in[15]). In any case, the most likely solution to the reggeon field theory with its infinite number of interaction terms will exhibit a critical behavior: this makes critical reggeon field theory the most promising candidate.

After this brief excursion into the Regge limit of QCD I now return to the small-x region of deep-inelastic scattering. I will try to illustrate that the improvement ideas of Gribov, Levin, and Ryskin[5] provide a "bridge" between the standard QCD-ladders[6] (Fig. 1) and the reggeon field theory. Starting from moderately small x (say 0.1) and keeping $Q^2 \gg \Lambda^2$ fixed, the region of decreasing x can roughly be divided into four different domains. In the first one the standard QCD-ladder diagrams (which are equivalent to the Lipatov-Altarelli-Parisi equations) provide a good description, down to about $x = 10^{-2}$. For such x, the ladders are dominated by gluons, and quark contributions can be neglected. One of the most promiment features of these diagrams is the ordering of internal

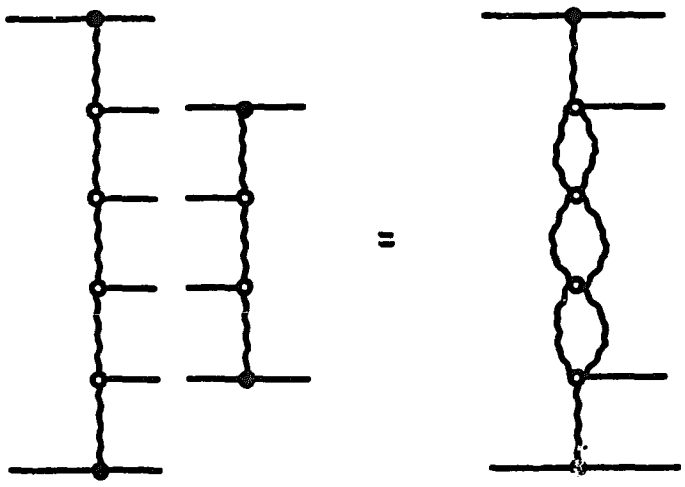

Fig. 4: A reggeon diagram: unitarity correction to a multiparticle production amplitude.

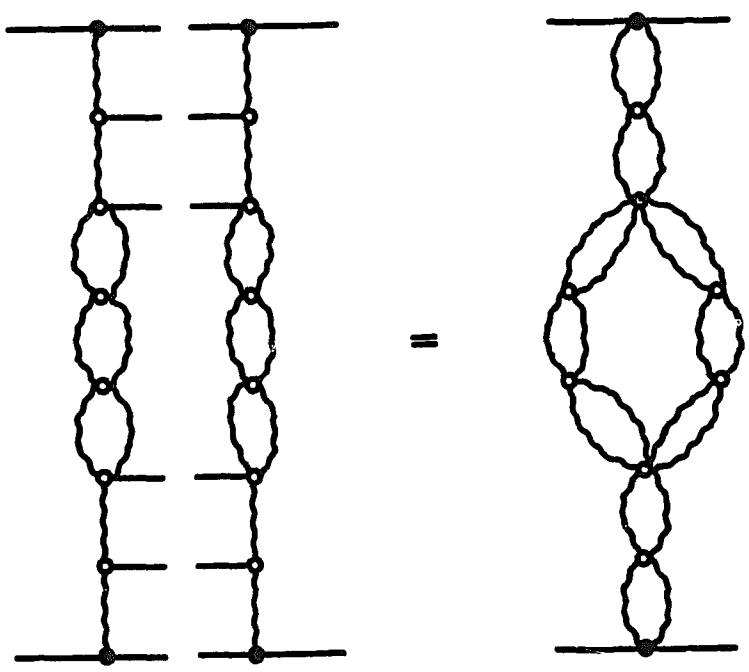

Fig. 5: A reggeon diagram: beyond the leading-lns approximation of the $2 \to 2$ scattering amplitude.

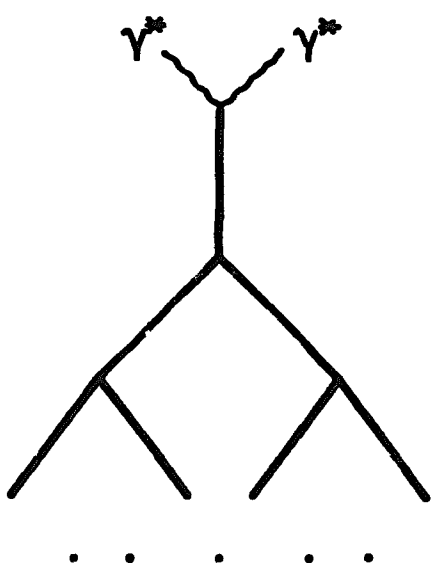

Fig. 6: A fan diagram: the black lines denote sums of ladder diagrams of fig. 1.

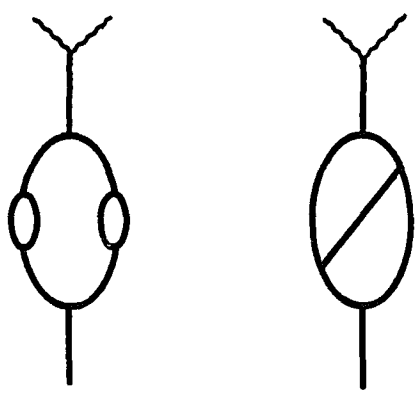

Fig. 7: More diagrams have to be included if one goes to smaller values of x: examples of "enhancement" diagrams.

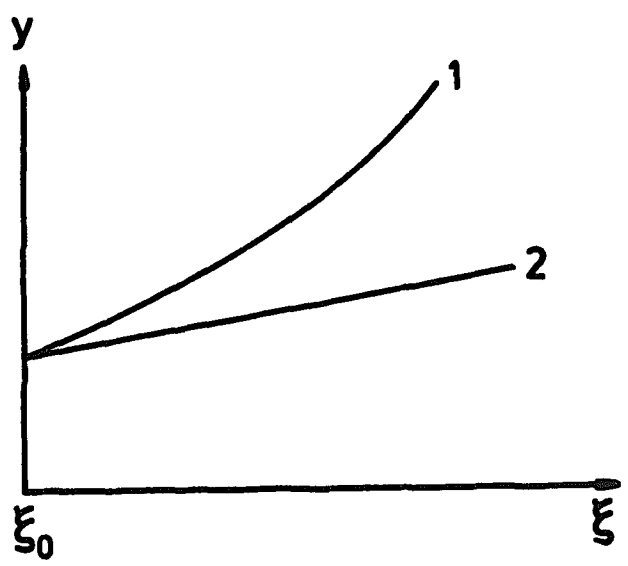

Fig. 8: Border lines in the ξ-y plane ($\xi = \ln\ln(Q^2/\Lambda^2)$).

momenta: the main contribution comes from those parts of the phase space where the fractions of longitudinal momentum decrease from 1 at the bottom to $x = Q^2/2pq$ at the top of the diagram, and the squares of four momenta $q_i^2 \approx q_i^2$ increase from some low hadronic scale Q_0^2 ($\sim$ few GeV^2) inside the incoming hadron up to the large scale Q^2 at the photon vertex. This ordering of internal momenta is one of the crucial differences between the QCD-ladders in deep-inelastic scattering and the ladder diagram (Fig. 2) of the leading-lns Pomeron: it protects the internal momenta from getting close to the IR-region where the coupling would become strong. Non-perturbative contributions are therefore restricted to the bottom part of the ladder diagrams, and, via factorization, they can be absorbed into the low-momentum hadronic wave function. In contrast to this, in the leading-lns Pomeron ladders the internal momentum integration includes the IR-region, and this part of the integration has even strong influence on the formation of the unwanted fixed-cut singularity. It therefore seems as if in the Regge limit there is no clean separation between large-momentum (perturbative) and low-momentum (nonperturbative) contributions. Another difference between the ladders of Fig. 1 and Fig. 2 is the reggeization of the gluon lines along the sides of the ladders: in Fig. 1 the contributions which lead to the reggeization are not yet needed.

When x becomes smaller the structure functions obtained from the QCD-ladders of Fig. 1 increase too strongly (eq. (1.1)), and further perturbative contributions have to be included, the so-called fan-diagrams shown in Fig. 6. They are built from the ladders of Fig. 1, and when moving from the top to the bottom, the number of ladders never decreases. They are discussed and analysed in Refs. 5 and 6; the first fan-diagram has also been carefully studied by A.H. Mueller and Qiu[7]. I only mention a few important features. The fan-diagrams are higher-twist contributions. The first fan-diagram, for example, has a factor $1/q_i^2$ (compared to the ladder of Fig. 1), where q_i^2 is the four momentum square associated with the branching vertex. At low x, this suppression factor is balanced by the increase in $1/x$ of the QCD-ladders. The main effect of the fan diagrams is to decelerate the growth in $1/x$ of the structure function at small x. More intuitively, as a result of the interaction between the large number of chains of parton decays, the density of very slow partons decreases. Comparison of the fan diagrams in Fig. 6 with the reggeon field theory clearly shows strong similarity: the fan diagrams present a subset. There is , however, still the difference due to the momentum ordering, i.e. the fan diagrams for deep-inelastic scattering are evaluated in a slightly different region of internal integration compared to the reggeon diagrams of Figs. 2, 4 or 5 (reggeization of the gluons, on the other hand, should now be included into the fan-diagrams). An important feature of the fan diagrams is the validity of the Abramovsky - Gribov - Kancheli cutting

rules[18] (AGK-rules). In order to obtain the DIS structure function, we are not interested in the full QCD-diagrams of Fig. 6 but only in their energy discontinuity. There are many contributions, but the different ways in which these diagrams can be cut are related through very simple counting rules[5] (diffractive cut: multiperipheral cut: double multiperipheral cut = 2 : -8 : 4). These cutting rules play an important role in the derivation of the Pomeron structure function (see below). Finally, for practical purposes one needs convenient methods for evaluating the sum of these fan diagrams. The authors of [5] present an integral equation which is (approximately) equivalent to a partial differential equation[5]. Alternatively, it is possibe to use a modified Altarelli-Parisi equation[17]. As I discuss further below, no serious attempt has been made so far to perform numerical studies of these fan diagrams.

When $^1/x$ increases further, then, according to Ref. 5, there is a region in x where the set of diagrams has to be further enlarged: in addition to the fan-diagrams one has to include the so-called enhanced diagrams (Fig. 7). This is a further step towards the reggeon field theory described above, but there is still the distinction connected with the momentum ordering. Also, since in DIS the variables are $^1/x$ and $\xi(= \ell n \ell n Q^2)$ rather than s and t, the expressions for the "bare propagators" of the ladders of Fig. 7 are different from those of corresponding reggeon diagrams. In fact, the actual form of the "energy-momentum" relation of the "reggeon field theory" in Fig. 7 has so far made it impossible to perform computations within this field theory (not to speak of finding its solution).

Ultimately, when $^1/x$ becomes asymptotically large, the theoretical description of the DIS structure function must coincide with the reggeon field theory. For this to happen, we still have to cross one last barrier: the ordering of momentum scales q_i^2 has to disappear, and this brings back all the problems with the infrared region and possible nonperturbative contributions which I have mentioned before. So it is at this stage that we are crossing the border line between perturbative and nonperturbative QCD.

This concludes my brief description of the interrelation of the small-x region in deep-inelastic scattering with the Regge limit (Pomeron) in QCD. Although the latter one is dominated by certain nonperturbative aspects which we do not yet understand, we can nevertheless say that the perturbative small-x description nicely matches the reggeon field theory (or at least that part of it which we know reliably). This survey also indicates that in the small-x region nonperturbative effects come in rather late: there is first the region where the (perturbative) fan-diagram description applies, and then, according to Ref. 5, another region where the enhanced diagrams of Fig. 7 are relevant. Comparing these theoretical ideas with experimental data will certainly provide a very

detailed test of QCD.

3. PHENOMENELOGY

After this theoretical overview I now turn to a few phenomenological topics. Most important, in my view, is the question for what range in x (at fixed Q^2) should one use the fan-diagrams, and where, finally, are the nonperturbative effects coming in. I have no answer to the second question, but there are some hints that the fan diagrams can be tested at HERA. Another point of interest is the $1/\sqrt{x}$ behavior of $xG(x,Q^2)$ at small x, which has been suggested some time ago[19]. Finally, I want to say a few words about the Pomeron structure function[20] and its relation to perturbative QCD.

I begin with the first question. The main point I want to make is that there in a good chance for HERA to test the fan diagrams of Ref. 5. But much more (theoretical) work needs to be done before the experiments start. Let me briefly summarize what is presently known. In Fig. 9 I illustrate how the authors of Ref. 5 describe the situation. In the Q^2-x plane there are two border lines, 1 and 2. Their equations are (eqs. (2.117b) and (2,119) of Ref. 5)

$$y = \ln(1/x) = \frac{0.21\ (\frac{11}{3}N - \frac{2}{3}n_f)}{8N}\ \ell n^2\ \frac{Q^2}{\Lambda^2} \qquad (N = 3) \qquad (3.1)$$

$$y = \ln(1/x) = \frac{0.21\ (\frac{11}{3}N - \frac{2}{3}n_f)}{4N}\ \ell n^2\ \frac{Q_0^2}{\Lambda^2} \cdot \ell n \ell n\ \frac{Q^2}{\Lambda^2} \qquad (3.2)$$

respectively. According to the discussion in Ref. 5, below line 2 lies the region where the standard-QCD description is applicable. Between 1 and 2 one should use the fan diagrams, and above line 1 we are in the regime of, first, the enhanced graphs of Fig. 7, than the reggeon field theory with its nonperturbative contributions. Since we do not exactly know where the latter starts, line 1 has to be taken as the lower limit (in $1/x$) for the onset of nonperturbative effects. In Fig. 9 I show a few examples[21] of eqs. (3.1) and (3.2); in order to make line 2 tangential to line 1 at the low-momentum point Q_0^2, we use, instead of (3.2), the equation

$$y = \ln(1/x) = \frac{0.21\ (\frac{11}{3}N - \frac{2}{3}n_f)}{8N}\ \ 2\ell n^2\ \frac{Q_0^2}{\Lambda^2}\ \ell n\ \frac{\ell n\ \frac{Q^2}{2}}{\ell n\ \frac{Q_0^2}{\Lambda^2}} + \ell n^2\ \frac{Q_0^2}{\Lambda^2} \qquad (3.2')$$

The estimates are rather sensitive to the choice of the low-momentum scale Q_0^2. The results indicate that already for $x \lesssim 10^{-2}$ the standard-QCD description should be replaced by the fan-diagrams. One should, however, keep in mind that eqs. (3.1) and (3.2) are derived by making certain approximations. A more refined analysis

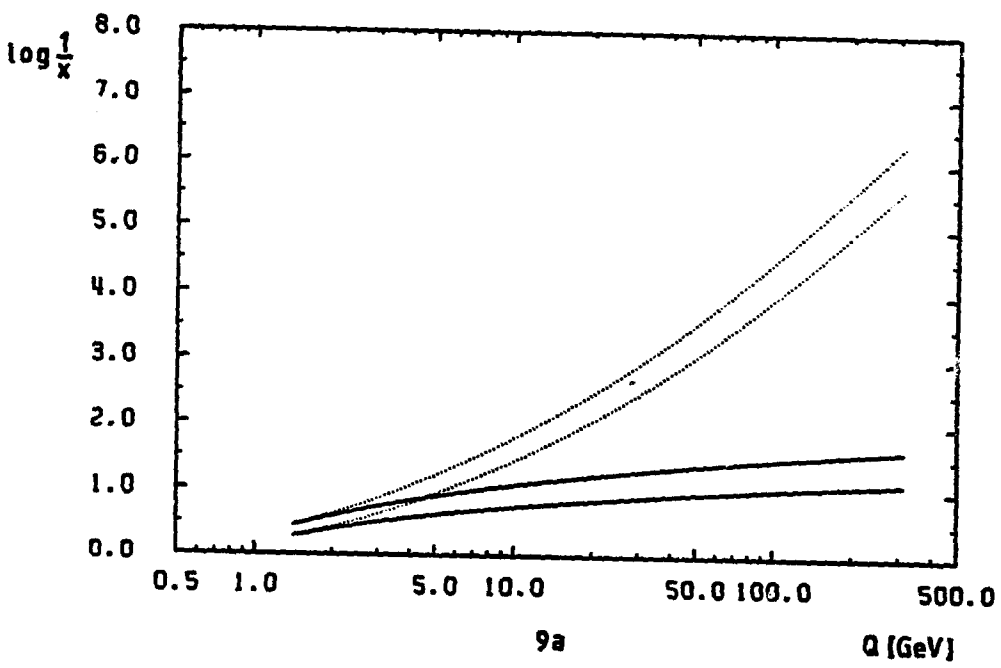

9a

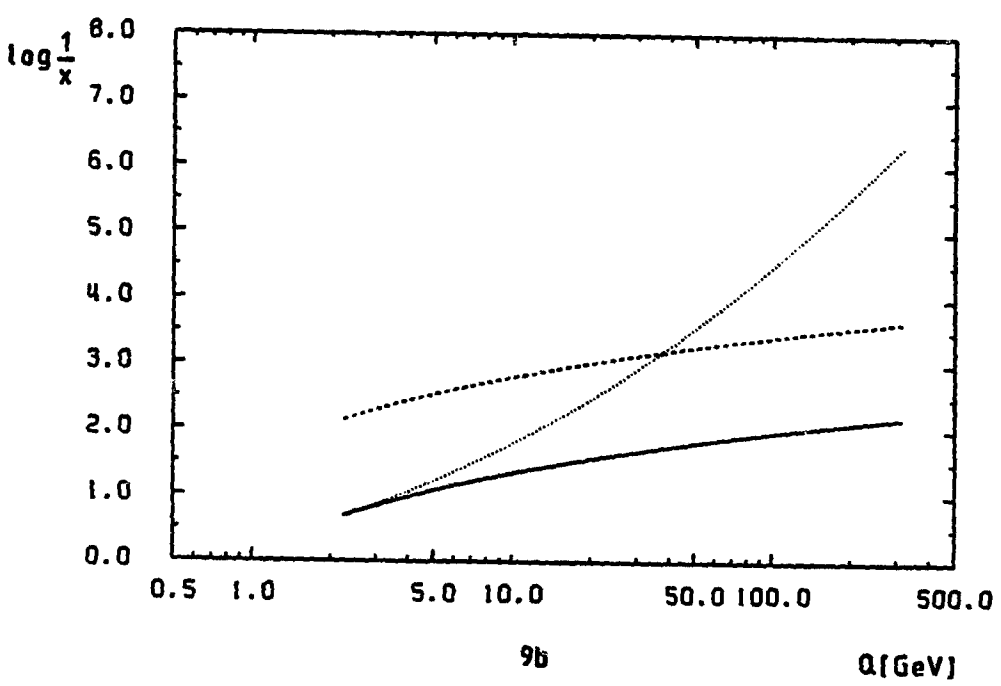

9b

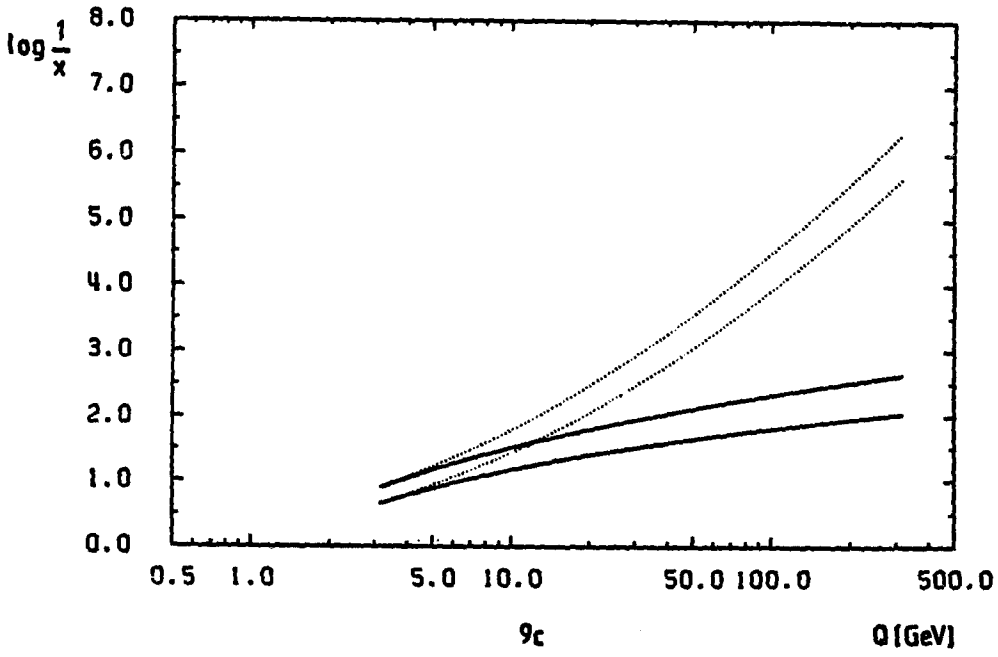

9c

Fig. 9: Plots of line 1 (eq. (3.1); dotted) and line 2 (eq. (3.2'); drawn) for different values Q_0^2 and Λ^2: (a) $Q_0^2 = 2$ GeV^2, $\Lambda = 0.2$ GeV (upper curves) and $\Lambda = 0.3$ GeV (lower curves). (b) $Q_0^2 = 5$ GeV^2, $\Lambda = 0.2$ GeV. (c) $Q_0^2 = 10$ GeV^2, $\Lambda = 0.2$ GeV (upper curves) and $\Lambda = 0.3$ GeV (lower curves). In case (b) we also show the line eq. (3.2) (dashed curve) which lies above that of eq. (3.2').

may slightly change the limiting curves shown in Fig. 9. In particular, one expects that the sensitivity to the choice of Q_0^2 disappears. In any case, given the fact that HERA reaches the interesting domain of small-x values, it is very important to perform a numerical calculation of the fan diagrams, i.e. to compare their small-x behavior with that of the standard QCD-ladder diagrams. To the best of my knowledge, this has not yet been done (for a first step in this direction see [22]). As a particular aspect of such an analysis, one will face the task of separating the effect due to the fan-diagrams from the uncertainty in the x-distribution at low Q_0^2 of the standard QCD evolution picture[23].

Another numerical estimate is due to J. Kwieciński[24]. Making a few simple assumptions about the coupling to the nucleon he has calculated the size of the first fan diagram (screening correction) relative to the standard QCD-ladder. The main result is that for $10 \leq Q^2 \leq 10^4$ GeV^2, the first fan diagram reaches about 10% of the standard ladder when x is of the order of 10^{-4}. He also computes the interaction probability of the partons

$$W(x,Q^2) = \frac{3\pi\alpha(Q^2)}{Q^2} \cdot \frac{xG(x,Q^2)}{R^2} \tag{3.3}$$

which has to be well-below 1 in order to make the single-ladder approximation work. For example, $W = 0.5$ for $Q^2 = 10$ GeV^2 and $x = 10^{-4}$, and $W = 0.1$ for $Q^2 = 100$ GeV^2 and $x = 10^{-4}$. The conclusion of this study seems to be that the physics of the fan diagrams sets in at somewhat lower x-values than it has been indicated by the authors of Ref. 5. But even then it may be possible to see first effects at HERA, and a numerical evaluation of the fan diagrams is needed. A much more pessimistic argument has been made by Mueller and Qiu[17]. They argue that the first fan diagram will be of the same order as the ladder if

$$\frac{\pi\alpha(Q^2)}{Q^2} \cdot \frac{xG(x,Q^2)}{R^2} = 1. \tag{3.4}$$

Comparing this with (3.3) and the calculation of Ref. 24 one immediately sees that either Q^2 has to be suspicously small or $1/x$ has to be exceedingly large (note the difference in the factor 3 between (3.3) and (3.4)). Given the other two estimates, it seems that the condition (3.4) may be a bit too strong.

Some years ago J.C. Collins[19] suggested that at small-x the gluon distribution $G(x_1Q^2)$ should increase more strongly than $1/x$, namely like $1/x^\alpha$ with $\alpha \gtrsim 1.5$. I cannot discuss to what extent this behavior has been successful in phenomenological applications, but I only want to comment on its justification within QCD. As the main theoretical basis of such a strong divergence in $1/x$, it has been argued that the small-x behavior of the standard ladder diagrams (Fig. 1) should be described by the leading j-plane singularity of the leading-lns Pomeron

(Fig. 2). (In fact, T. Jaroscewicz[25] used the correspondence between the ladder diagrams in Figs. 1 and 2 to calculate the anomalous dimension $\gamma_+(n)$ beyond the leading order in α_s. As a result of the higher order corrections, the singularity in n of $\gamma_+(n)$ shifts from $n = 1$ to $n = \alpha_c \approx 1.5$. A more recent discussion of the Lipatov integral equation for the diagrams of Fig. 2, and its implications for the small-x behavior of the structure function has been given by Collins and Kwieciński in [26].) As I have explained in the first part of my talk, the leading singularity of the diagrams in Fig. 2, in my opinion, has little significance. Rather than summing these diagrams to all order in α_s (and thereby entering regions of internal phase space where perturbation theory is unreliable), one has to take into account more and more of the s-channel unitarity corrections (i.e. reggeon diagrams with more than 2 reggeized in the t-channel). If, on the other hand, one wants to start from the standard ladders (Fig. 1) and then more on towards smaller and smaller x-values, the investigations of Ref. 5 clearly state that it is not allowed to simply extrapolate from Fig. 1 to Fig. 2. One rather has to proceed from Fig. 1 to the fan-diagrams of Fig. 6 and the enhanced diagrams of Fig. 7 to the full reggeon field theory (Fig. 5). I therefore conclude that the leading singularity of the ladders in Fig. 2 cannot be used to justify the $1/x^{\alpha}$-behavior of $G(x,Q^2)$. Very unfortunately, this insight does not yet answer the question what x-distribution should be used as starting point in the standard QCD evolution analysis, in particular what kind of small-x behavior. At low Q^2, the small-x region is really the Regge-limit, i.e. inaccessible to perturbative QCD. It seems to me that the best we can do at the moment is to use some functional dependence in $1/x$ which reflects the observed rise of the hadronic total cross section. Subsequent Q^2-evolution then has to proceed in accordance with the restrictions discussed before (as illustrated in Fig. 8), and it will lead to some modified small-x behavior at higher Q^2-values.

My final topic is the Pomeron structure function and its interpretation within QCD. First of all, as I will make clear, it provides a certain test of the ideas which I have explained in the first part. Secondly, there is a connection between the Pomeron structure function and other known hadronic structure functions, which has not yet received much attention. The idea of defining a Pomeron structure function goes back to Ingelman and Schlein[20] who suggested to look for two large-transverse-momentum jets inside a diffractively produced high missing-mass cluster (Fig. 10a and b). Suggestions in the same direction were also made by Fritzsch and Streng[27], and theoretical aspects where discussed by Berger, Collins, Soper and Sterman[28] and Donnachie and Landshoff[29]. By analogy with the Regge analysis of the triple-Regge inclusive cross section (Fig. 10a), the following expression has been suggested[20]:

$$\frac{d^2\sigma_{jj}}{dtdM^2} = \frac{6.8}{M_X^2}\left[e^{5.6t} + 0.04e^{2t}\right] \cdot \frac{\int dx_1 dx_2 \sum_{i,k} G_{\mathbb{P}k}(x_2,Q^2) f_i(x_1,Q^2) \frac{d\hat{\sigma}_{ik}}{dt}}{\sigma_{p\mathbb{P}\to X}} \qquad (3.5)$$

where $G_{\mathbb{P}}(x,Q^2)$ defines the (gluonic) Pomeron structure function. In this picture, the Pomeron is viewed as an "incoming particle" which can be handled in very much the same way as a normal hadron. More recently[30] UA8 data have been analysed and compared to (3.5), and agreement has been found for $x \cdot G(x,Q^2) = 6 \cdot (1-x)^5$ ("soft Pomeron structure function"). In Fig. 11 I illustrate how the Pomeron structure function can be measured at HERA: one lookes for events with a large rapidity gap between the elastically scattered proton and a high-missing-mass cluster in the direction of the high-Q^2 photon.

When analysing these processes within QCD, one arrives at expressions[5] which are somewhat different from those based on the triple-Regge analog. This difference is easily seen when one applies the QCD evolution picture to the process in Fig. 11a or b. In order to have an interaction with the high-Q^2 photon, we need far-off shell quarks and gluons which have to evolve from the low momentum constituents inside the scattering hadron. Most naturally, one would expect that this evolution should start already inside the Pomeron, such that at the triple-vertex in Fig. 11b the momentum scale q^2 lies somewhere between the starting low-momentum Q_0^2 and the final high momentum square Q^2. Since this scale q^2 is not fixed, one has to integrate over q^2. As illustrated in Fig. 11b, the cross section for this semiinclusive reaction represents a special contribution to the energy discontinuity ("diffractive cut") of the first fan diagram. Because of the counting rules alluded to before, this cut is in magnitude (not in sign) equal to the contribution of the fan diagram to the deep-inelastic structure function. This leads to the following expression for the Pomeron structure function[5] and the inclusive cross section:

$$\frac{d^2\sigma}{dtdM^2} = \frac{\text{const}}{M^2}\int_{Q_0^2}^{Q^2} dq^2 \tilde{\phi}\left(\frac{x}{x_M},Q^2,q^2\right)\alpha_s^2(q^2) g \quad \phi^2(x_M,q^2,t) \qquad (3.6)$$

Here $x_M = \frac{M_X^2+Q^2}{s+Q^2}$; $\tilde{\phi}(x/x_M,Q^2,q^2)$ and $\phi(x_M,q^2)$ stand for (mainly gluonic) QCD structure functions, and $\alpha_s^2(q^2)\cdot g$ denotes the triple-vertex. The normalization of (3.6) is not free; it is, at least in principle, calculable from standard QCD ingredients. The variable q^2 is the momentum scale at the triple-vertex: it is this integration over q^2 which is missing in the expressions coming from the triple-Regge analogy (eq. (3.5)). There it was assumed that the Pomeron is the same as in hadron-hadron scattering, i.e. q^2 is small. Equation (3.6) suggests that there

may be contributions coming from a "hard Pomeron" with a large momentum scale q^2.

In order to decide how well (3.6) works and whether (3.5) can be viewed as a valid approximation to (3.6), one has to do a numerical analysis of (3.6). Since Fig. 11b represents a higher-twist contribution $\sim 1/q^2$ to the structure function, there seems to be a strong enhancement of the integral in the low-q^2 region. However, depending upon the values for x_M, Q^2, x, there may be a more subtle balance between the different parts of the integrand. G. Ingelman and myself[31] have started a first numerical study of this question. Using a simpler version of (3.6) (we use the expressions of Kwieciński[24], making the assumption that all ingredients of (3.6) are dominated by gluons) we have studied the q^2-dependence of the integrand of (3.6), taking different sets of values for x_M, Q^2 and x. Two (preliminary) curves are shown in Figs. 12a and b. In Fig. 12a we plot the integrand versus q^2 ($Q^2 = 50$ GeV^2, $x_M = 0.05$, $x = 5 \cdot 10^{-4}$) (note that the overall normalization is fixed). As expected, there is a strong peaking at low q^2-values. The by far strongest contribution comes from $q^2 < 5$ GeV^2, where perturbative QCD becomes unreliable. This entirely justifies the use of (3.5). Note, however, that a rather naive extrapolation of the drawn curve down to $q^2 \approx 1$ GeV^2 leads to a nice agreement with the numerical values used by Bonio et al.[30]. Starting from values of q^2 where perturbative QCD allows to calculate the integrand of (3.6), one could have almost "predicted" the (low-q^2 dominated) Pomeron structure function used in[20]. In Fig. 11b we show the same curve for a different set of values ($Q^2 = 50$ GeV^2, $x_M = 0.05$, $x = 0.045$; note that this still corresponds to values of M_X^2, s/M_X^2 for which triple-Regge kinematics is valid). Here the situation is different, in that large q^2-values are dominating: one is no longer probing the "soft" Pomeron of hadron-hadron scattering. These two (extreme) examples illustrate that in some (but not all) cases (3.5) can be used as a valid approximation to (3.6): the function G , together with the other triple-Regge parameters in (3.5), represent the low-q^2 extrapolation of known QCD structure functions. In other cases, the Pomeron structure function can be calculated directly from (3.6). There is certainly more work to be done to make full use of (3.6) and have a further test of QCD.

4. CONCLUSION

Let me finally try to summarize . In the first part I have tried to make clear that a nice consistency has emerged between the small-x limit of deep-inelastic scattering and the Regge-limit. This can be stated although our understanding of the nonperturbative aspects of the Regge limit is not complete. Phenomenologically, I think the most important aspect is that HERA (and, later on, SSC) does have a good chance to test the beginning of the fan diagrams: this, however, needs further

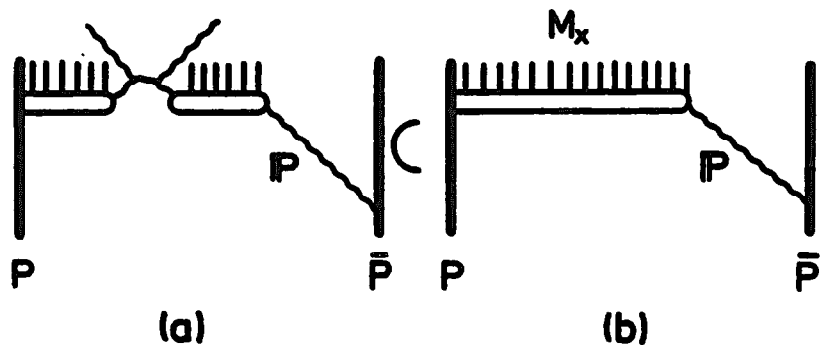

Fig. 10: The Ingelman-Schlein final state configuration for the Pomeron structure function: (a) two large transverse momentum jets inside the diffractively produced missing mass, (b) the inclusive reaction $\bar{p}p \to \bar{p} + M_X$.

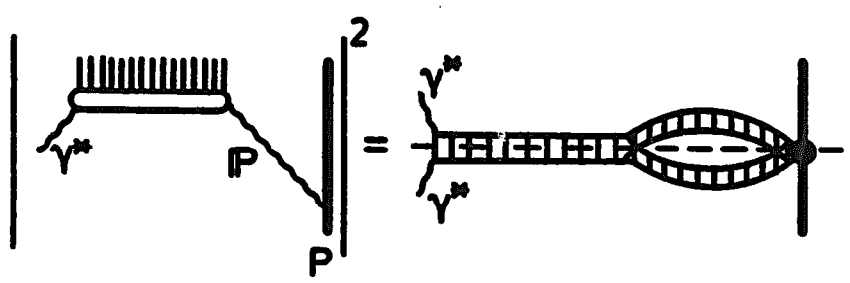

Fig. 11: The Pomeron structure function in deep inelastic scattering.

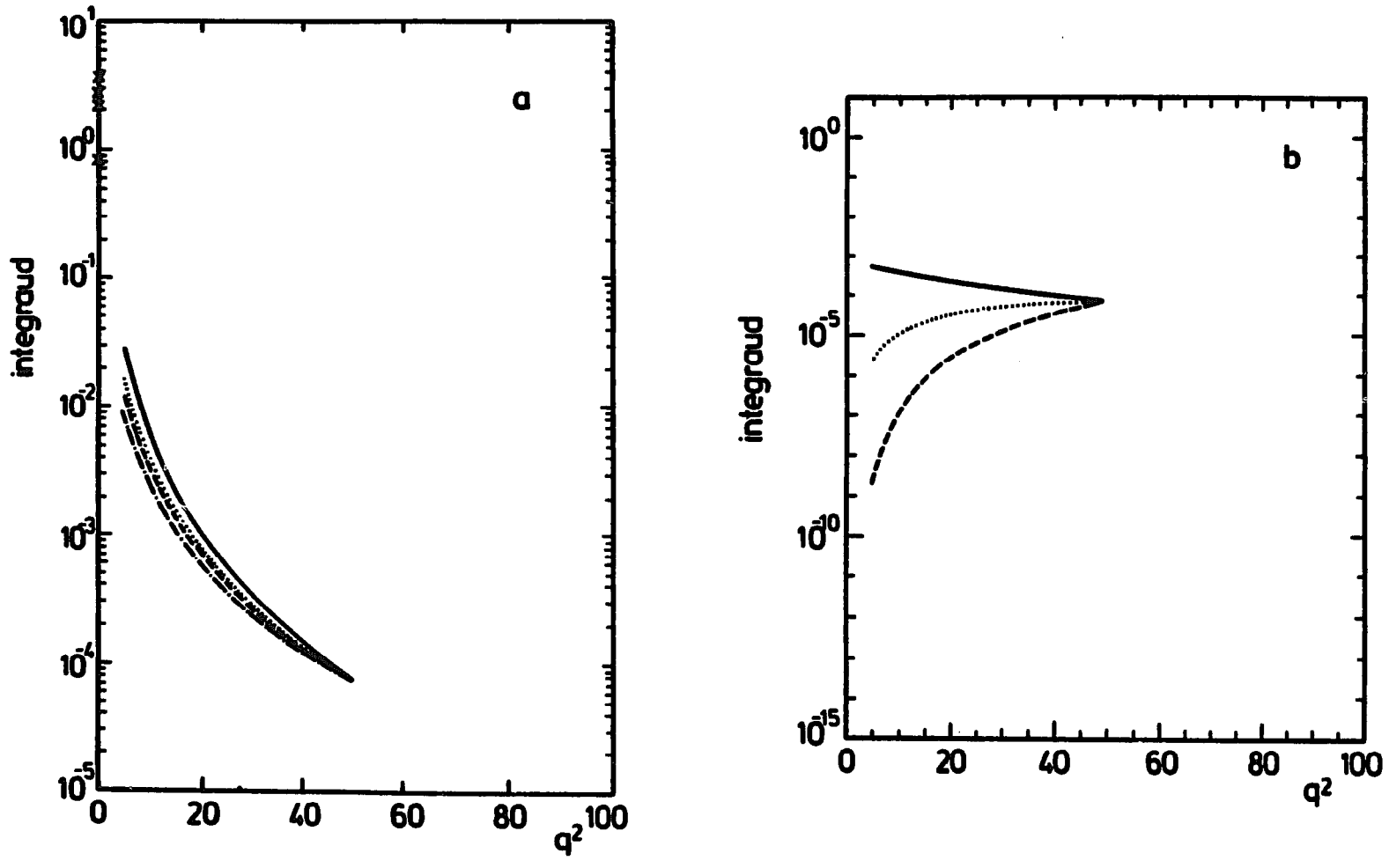

Fig. 12: A plot of the integrand of eq. (3.6) (for $\tilde{\phi}$, ϕ, and $\alpha_s^2 g$ we use the expressions of Ref. 24). We take $Q^2 = 50$ GeV^2, $x_M = 0.05$. For $z = x/x_M$ we use: (a) 0.01 (drawn line), 0.05 (dotted), 0.1 (dashed), 0.25 (dotted-dashed); (b) 0.5 (drawn), 0.75 (dotted), 0.9 (dashed). In Fig. 12a the crosses on the vertical axis denote the values used in Ref. 30 (eq. (3.5)).

heoretical work which should be done before HERA comes into operation. I also believe that the Pomeron structure function provides a test of our understanding of QCD: it can be measured both at the $Sp\bar{p}S$-collider and at HERA.

ACKNOWLEDGEMENT

I would like to thank M. Block and A. White for inviting me to this pleasant and stimulating conference.

REFERENCES

1) "Proceedings of the 1984 Summer Study on the Design and Utilization of the Superconducting Supercollider, Snowmass 1984", New York, AIP 1985 (ed. R. Donaldson and J.C. Morfin): L. Durand, p. 256, L. Durand, p. 258; P.W. Johnson and Wu-ki Tung, p. 260
2) J.C. Collins, ibidem p. 251
3) "Proceedings of the 1986 Summer Study of the Physics of the Superconducting Super Colliders, Snowmass 1986, New York, APS 1986 (ed. R. Donaldson, J. Marx): Wu-ki Tung, p. 70; D.W. McKay and J.R. Ralston, p. 72
4) Proceedings of the Madison Conference 1986: "Physics Simulations at High Energies", (ed. V. Barger, T. Gottschalk and F. Halzen, World Scientific, Singapore 1987)
5) L.V. Gribov, E.M. Levin, M.G. Ryskin, Phys. Rep. 100 (1983), 1
6) For general reviews see: C.H. Llewellyn Smith, Schladming Lectures 1987, Acta Physics Austr., Suppl. XIX (1978), 331; Yu. Dokshitzer, D.I. Dyakovov, S.I. Troyan, Phys. Rep. 58 (1980), 269; E. Reya, Phys. Rep. 69 (1981), 195; A.H. Mueller, Phys. Rep. 73 (1981), 237
7) E.A. Kuraev, L.N. Lipatov, V.S. Fadin, Sov. Phys. JETP 44 (1976), 443
8) E.A. Kuraev, L.N. Lipatov, V.S. Fadin, Sov. Phys. JETP 45 (1977), 199
9) Ya.Ya. Balitzky, L.N. Lipatov, Sov. Journ. Nucl. Phys. 28 (1978), 822
10) Ya.Ya. Balitzky, L.N. Lipatov, JETP Lett. 30 (1979), 355
11) L.N. Lipatov, Sov. Phys. JETP 63 (1986) 904
12) V.S. Fadin, contribution to this conference, and V.S. Fadin, L.N. Lipatov, Novosibirsk Preprint 89-13
13) For numerical studies of the Lipatov integral equation see: G.J. Daniell and D.A. Ross, Southampton preprint SHEP 88/85-5 P.A. Raczka and M. Pindor, Trieste preprint IC/88/362
14) J. Bartels, Nucl. Phys. B151 (1979), 293; Nucl. Phys. B175 (1980), 365; Acta Physica Polonica B11 (1980), 281; unpublished
15) A.R. White, contribution to this conference and references therein
16) L.V. Gribov, E.M. Levin, M.G. Ryskin, Nucl. Phys. B188(1981), 555 and Ref. 4).
17) A.H. Mueller and J. Qiu, Nucl. Phys. B268 (1986), 427
18) V.A. Abramowvsky, V.N. Gribov, O.V. Kancheli, Yad. Fiz. 18 (1973), 595 (Sov. Journal Nucl. Phys.)
19) J.C. Collins, "Semihard processes and QCD", in Ref. 4, p. 265
20) G. Ingelman and P. Schlein, Phys. Lett. 152B (1985) 256
21) J. Bartels and G. Schuler, unpublished
22) J.P. Ralston and D.W. McKay, in Ref. 4), p. 30
23) For numerical studies of the evolution in Q^2 of different low-x behaviors within the standard-QCD ladders see, for example: E. Eichten, I. Hinchliffe, K. Lane, C. Quigg, Rev. Mod. Phys. 56 (1984), 579 M. Glück, R.M. Goodbole, E. Reya, Zeitschr. f. Physk C41 (1989), 667
24) J. Kwiecińsky, Zeitschr. f. Physik C29 (1985), 147
25) T. Jaroscewicz, Phys. Lett. 116B (1982), 291
26) J.C. Collins and J. Kwiecinsky, Nucl. Phys. B316 (1988), 307

27) H. Fritzsch and H.H. Streng, Phys. Lett. 164B (1985), 391
28) E.L. Berger, J.C. Collins, D.E. Soper, G. Sterman, Nucl. Phys. B286 (1987), 704
29) A. Donnachie, P.C. Landshoff, CERN-TH.5020/88
30) R. Bonino et al., Phys. Lett. 211B (1988), 239
31) G. Ingelman and J. Bartels, DESY-preprint in preparation.